Asian Journal of Chemistry; Vol. 36, No. 5 (2024), 1126-1134

ASIAN JOURNAL OF CHEMISTRY

https://doi.org/10.14233/ajchem.2024.31241

Synthesis and Evaluation of Aminothiazole Hybrids as Potential Acetylcholinesterase Inhibitors

ARTI SONI[1,*], ASHWANI KUMAR[1], VIVEK KUMAR[2], RAVI RAWAT[3] and VOLKAN EYUPOGLU[4]

[1]Department of Pharmaceutical Sciences, Guru Jambheshwar University of Science and Technology, Hisar-125001, India
[2]Janta College of Pharmacy, Butana, Sonipat-131001, India
[3]School of Health Sciences & Technology, UPES University, Dehradun-248007, India
[4]Department of Chemistry, Cankiri Karatekin University, Cankiri-18100, Turkey

*Corresponding author: E-mail: artisoni26@gmail.com

Received: 16 January 2024; *Accepted*: 28 March 2024; *Published online*: 30 April 2024; AJC-21619

This study aimed to synthesize aminothiazole derivatives with 1,3,4-oxadiazole moiety and evaluated their acetylcholinesterase (AChE) and antioxidant activity in order to check their potency against Alzheimer's disease. Inhibition screening against AChE indicated that synthesized derivatives expressed well to moderate AChE inhibitory activity *in vitro*. Of the examined synthetic compounds (**3a-i**), compound **3d** expressed the best inhibition with IC_{50}-0.35 µM. The antioxidant activity of all the synthesized compounds was also analyzed by the DPPH assay. Finally, in molecular docking analysis, the best docking score was displayed by the most active compound **3d** supported the *in vitro* inhibition results. Compound **3d** emerged to be promising lead for the further development of anti-Alzheimer's drugs.

Keywords: Alzheimer's disease, AChE inhibition, Aminothiazole, Antioxidant, Molecular docking.

INTRODUCTION

Alzheimer's disease is a major neurodegenerative disease affecting especially aged people [1-3] and is characterized by short term memory loss, cognitive and language impairment [4]. Currently more than 55 million people have dementia worldwide, over 60% of whom live in low-and middle-income countries and nearly 10 million new cases are added every year [5]. Many pathophysiological causes have been identified in Alzheimer's disease like inflammation of neurons, deficiency of acetylcholine, oxidative stress, amyloid β aggregation, neurofibrillary tangles (abnormal accumulation of tau protein), *etc.* [6-8]. The approved therapy for Alzheimer's disease available today is capable to relieve symptoms only without curing disease's progression [9]. As the etiology of Alzheimer's disease is multifactorial, hence multifunctional drugs having complementary biological activities have been regarded as the best pharmacological choice [10,11].

The loss of acetylcholine level is responsible for the cognitive decline in Alzheimer's disease, which is associated with consistently raised level of acetylcholinesterase (AChE) around amyloid plaques regions [12,13]. The level of acetyl-choline can be enhanced by preventing its hydrolysis by AChE enzyme [14] and thus inhibition of AChE has remained significant approach in the management of cognitive and behavioural symptoms of mild and moderate stages of Alzheimer's disease.

Oxidative stress either acute or chronic is also another major factor for the initiation and progression of Alzheimer's disease [15]. The chronic form of oxidative stress is more injurious and may result in the alteration of cell components, homeostasis and common degenerative diseases including Alzheimer's disease [16]. Free radicals actively damage peroxidizable fatty acids present in the brain and may result in the formation of new detrimental structures including amyloid-β, tau protein, *etc.* [17]. Accumulation of amyloid-β peptides triggers the pathogenesis of Alzheimer's disease due to neuronal damage [18]. Therefore preventing amyloid-β oligomer formation using the antioxidant feature can be another approach for discovery of new drugs against Alzheimer's disease.

Thiazole is a versatile and valuable scaffold in design of novel compounds of medicinal importance *e.g.* anti-Alzheimer [19,20], anti-convulsants [21], anti-HIV [22], anticancer [23, 24], antifungal [25,26], anti-inflammatory [27], antioxidant [28] and neuroprotective [29]. The activity of thiazole is remarkably affected by the position and nature of substituents. Thiazole carry both an electron-donating group (-S-) and an electron

accepting group (C=N) and these create a stable heterocyclic compound [30,31].

The oxadiazole moiety is considered to have varied medicinal actions like anti-alzheimer [30,32], anti-inflammatory [33], antimicrobial [34], antimalarial [35], antidepressant [36], analgesic [37], anticancer [38] and antiviral [39], *etc*. Also, the multifunctional nature of the 1,3,4-oxadiazole nucleus with different substitutions has been reported for significant anticholinesterase and antioxidant activities [32,40]. The oxadiazole derivatives (Fig. 1) have been reported to have AChE inhibitory activity with IC_{50} = 1.098 µM and 50.87 nM, respectively.

Encouraged from aforementioned findings, herein we synthesized hybrid compounds using these scaffolds having the capability to maintain acetylcholine levels in the brain along with antioxidant activity. In this study, nine aminothiazole derivatives bearing (5-(pyridine-4-yl)-1,3,4-oxadiazol) (**3a-i**) moiety. Subsequently, the synthesized compounds have been evaluated for their *in vitro* anticholinesterase and antioxidant activity. The *in vitro* results were also supported by *in silico* binding affinity by glide dock.

EXPERIMENTAL

The synthesis reagents and solvents were acquired from SRL, S.D. Fine, HPLC, Hi-Media Pvt. Ltd., *etc*. and used without purification. The reaction progress was monitored by TLC plates made using silica gel G and the spots were visualized by UV chamber. FT-IR spectra were recorded on the Perkin-Elmer 1710. ^{1}H NMR (400 MHz) and ^{13}C NMR (101 MHz) spectra were recorded (Bruker Avance III FT-NMR spectrometer) in deuterated chloroform ($CDCl_3$) using tetramethylsilane (TMS) as an internal standard. High-resolution mass spectra (HRMS) were recorded on SCIEX TRIPLE TOF 5600 and the values are reported in *m/z*. The AChE enzyme from *Electrophorus electricus* (Sigma-Aldrich) was used for *in vitro* study.

General procedure for synthesis of 2-chloro-*N*-(4-phenylthiazol-2-yl)acetamide derivatives (2a-i)

Step-1: General procedure for the synthesis of 2-amino-4-phenyl-thiazole derivatives (1a-i): A solution containing 2 mmol of each respective acetophenone (**a-i**), 3 mmol of thiourea and 2 mmol of I_2, in the presence of triethylamine, was heated under reflux in ethyl alcohol for 6-7 h. The advancement of the reaction was monitored using thin-layer chromatography (TLC) with a solvent mixture of petroleum ether and ethyl acetate in a ratio of 4:1. The reaction mixture was cooled to room temperature and the solid was separated after the solvent was evaporated. The material was dissolved in water and then treated with ethyl acetate to eliminate any remaining unreacted I_2. The pH of aqueous phase was modified to pH 8 using NH_3, resulting in the formation of solid product [41]. The resultant solid product was purified by recrystallization using ethanol, resulting in a pure product.

Step-2: General procedure for synthesis of 2-chloro-*N*-(4-phenylthiazol-2-yl)acetamide derivatives (2a-i): A mixture of 0.05 mol of aminothiazole (dissolved in $CHCl_3$) and 0.05 mol of anhydrous K_2CO_3 was placed in a round-bottom flask for reflux at 80-85 ºC for 8-10 h. To this refluxing solution, 5 mL chloroacetylchloride solution (0.05 mol in $CHCl_3$) was added dropwise [42]. After completion of reflux reaction, excess chloroacetyl chloride was evaporated and the crude compound obtained was recrystallized with ethanol to get a pure product.

General procedure for the synthesis of compounds 3a-i

Step-3: General procedure for the synthesis of *N*-(4-(3-nitrophenyl)thiazol-2-yl)-2-((5-(pyridine-4-yl)-1,3,4-oxadiazol-2yl)thio)acetamide (3): Isoniazid (0.01 mol) was dissolved in ethanol along with KOH (0.01 mol) and CS_2 (20 mL) was added to it. The mixture was refluxed for 8-10 h using ethanol as solvent. After the reaction, cold distilled water and then dil. HCl was added to get the precipitate of the final product [43]. The solid product was separated, dried and the crude product was recrystallized from ethanol.

Step-4: General procedure for synthesis of *N*-(4-phenylthiazol-2-yl)-2-((5-(pyridin-4-yl)-1,3,4-oxadiazol-2-yl)thio)-acetamide derivatives (3a-i): Intermediate **2a-i** was refluxed for 6-8 h with an equimolar quantity of 5-(pyridine-4-yl)-1,3,4-oxadiazole-2-thiol (**3**) and K_2CO_3 (0.1 mol) in the presence of acetone to get respective product **3a-i** [43] (**Scheme-I**). The residue was washed with cold water, dried and the crude product was recrystallized from ethanol.

***N*-(4-(3-Nitrophenyl)thiazol-2-yl)-2-((5-(pyridine-4-yl)-1,3,4-oxadiazol-2yl)thio)acetamide (3a):** Yield: 72%; dark yellow solid; m.p.: 184-185 ºC; ^{1}H NMR (400 MHz, $CDCl_3$)

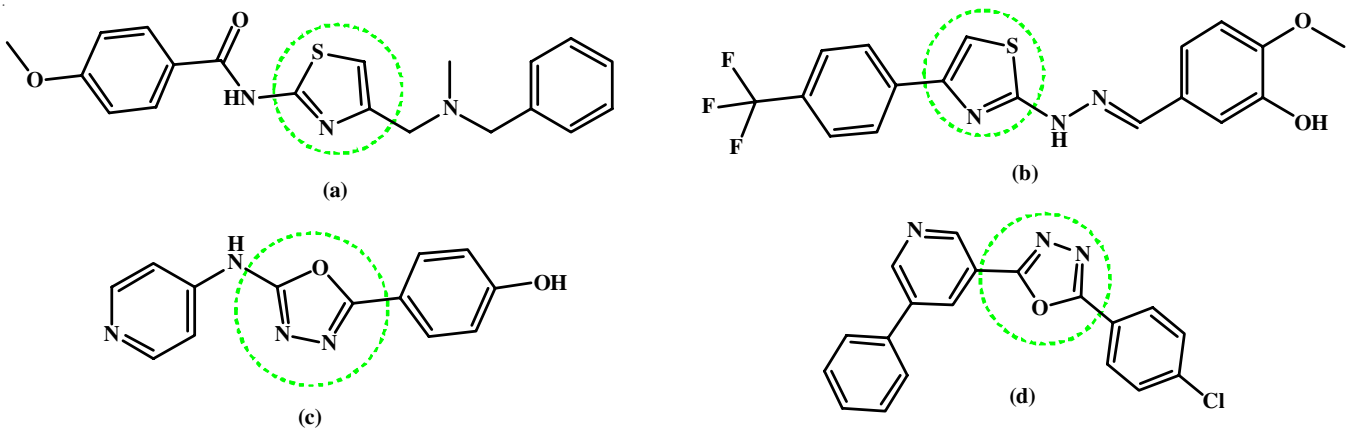

Fig. 1. Structures of previously reported AChE inhibitors having thiazole (a & b), 1,3,4-oxadiazole (c & d) scaffolds

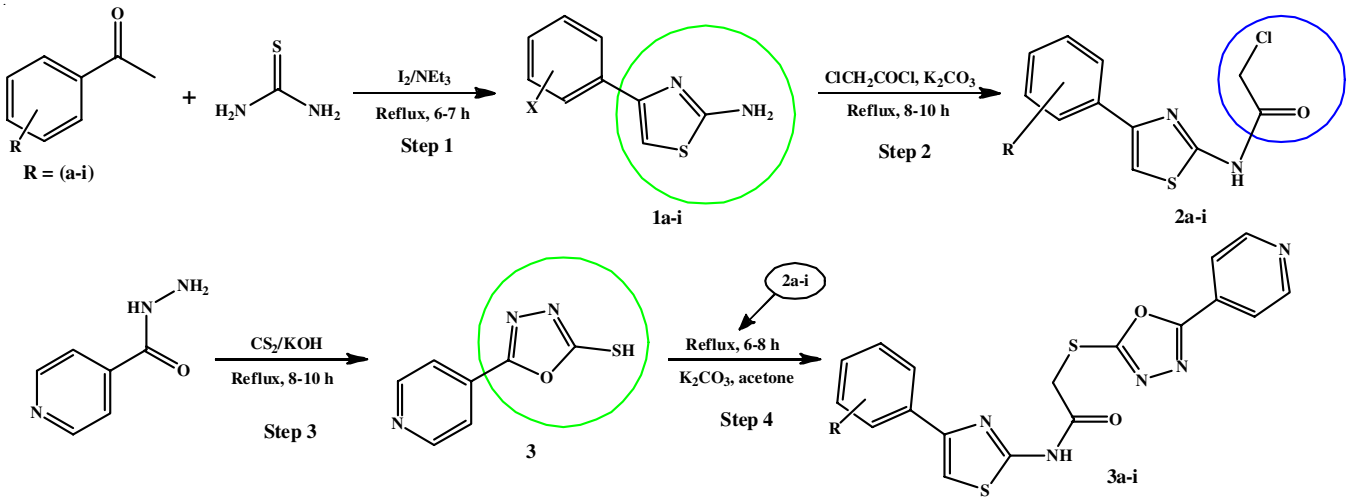

Scheme-I: Synthesis of thiacetamido thiazole derivatives

δ ppm: 12.72 (s, 1H, NH), 7.75-6.61 (m, 8H, Ar), 6.86 (s, 1H, CH of thiazole), 3.85 (s, 2H, CH_2); ^{13}C NMR (101 MHz, $CDCl_3$) δ ppm: 167.4, 164.3, 165.1, 150.2, 149.8, 146.4, 143.7, 133.8, 134.2, 128.1, 127.3, 121.9, 118.4, 102.9, 38.7; HRMS (ESI) *m/z* for $C_{18}H_{12}N_6O_4S_2$ calculated: 440.0405, found: 440.0410.

***N*-(4-(2,5-Dimethoxyphenyl)thiazol-2-yl)-2-((5-(pyridine-4-yl)-1,3,4-oxadiazol-2-yl)thio)acetamide (3b):** Yield: 78%; brown solid; m.p.: 195-197 ºC; ^{1}H NMR (400 MHz, $CDCl_3$) δ ppm: 13.35 (s, 1H, NH), 7.75-6.89 (m, 7H, Ar), 6.74 (s, 1H, CH of thiazole), 3.97 (s, 2H, CH_2), 3.89-3.91 (m, 6H, 2×OCH_3); ^{13}C NMR (101 MHz, $CDCl_3$) δ ppm: 167.8, 163.9, 164.3, 152.2, 151.1, 148.3, 143.43, 120.8, 118.9, 115.8, 104.7, 55.9, 38.3; HRMS (ESI) *m/z* for $C_{20}H_{17}N_5O_4S_2$ calculated: 455.3420, found: 455.3415.

***N*-(4-(4-Bromophenyl)thiazol-2-yl)-2-((5-(pyridine-4-yl)-1,3,4-oxadiazol-2-yl)thio)acetamide (3c):** Yield: 70%; dark yellow solid; m.p.: 185-187 ºC; ^{1}H NMR (400 MHz, $CDCl_3$) δ ppm: 12.34 (s, 1H, NH), 7.5-6.61 (m, 8H, Ar), 6.95 (s, 1H, CH of thiazole), 3.85 (s, 2H, CH_2); ^{13}C NMR (101 MHz, $CDCl_3$) δ ppm: 168.5, 165.1, 163.9, 150.6, 150.2, 138.7, 129.6, 122.3, 105.1, 38.3; HRMS (ESI) *m/z* for $C_{18}H_{12}BrN_5O_2S_2$ calculated: 473.1301, found: 473.1297.

***N*-(4-(2,4-Dichlorophenyl)thiazol-2-yl)-2-((5-(pyridine-4-yl)-1,3,4-oxadiazol-2-yl)thio)acetamide (3d):** Yield: 72%; light yellow solid; m.p.: 180-182 ºC; ^{1}H NMR (400 MHz, $CDCl_3$) δ ppm: 13.17 (s, 1H, NH), 8.74-7.49 (m, 7H, Ar), 6.58 (s, 1H, CH of thiazole), 3.90 (s, 2H, CH_2); ^{13}C NMR (101 MHz, $CDCl_3$) δ ppm: 168.4, 165.1, 162.8, 150.6, 150.2, 142.9, 131.5, 122.3, 105.4, 38.7; HRMS (ESI) *m/z* for $C_{18}H_{11}Cl_2N_5O_2S_2$ calculated: 464.3409, found: 464.3415.

***N*-(4-(2-Chlorophenyl)thiazol-2-yl)-2-((5-(pyridin-4-yl)-1,3,4-oxadiazol-2-yl)thio)acetamide (3e):** Yield: 74%; Beige solid; m.p.: 186-187 ºC; ^{1}H NMR (400 MHz, $CDCl_3$) δ ppm: 12.69 (s, 1H, NH), 737-6.89 (m, 8H, Ar), 6.62 (s, 1H, CH of thiazole), 3.97 (s, 2H, CH_2); ^{13}C NMR (101 MHz, $CDCl_3$) δ ppm: 167.8, 164.3, 162.8, 149.8, 143.7, 131.9, 129.2, 121.9, 103.3, 37.6; HRMS (ESI) *m/z* for $C_{18}H_{12}N_5ClO_2S_2$ calculated: 429.9841, found: 429.9845.

***N*-(4-(3,4-Dimethoxyphenyl)thiazol-2-yl)-2-((5-(pyridine-4-yl)-1,3,4-oxadiazol-2-yl)thio)acetamide (3f):** Yield: 77%; light yellow solid; m.p.: 170-172 ºC; ^{1}H NMR (400 MHz, $CDCl_3$) δ ppm: 13.35 (s, 1H, NH), 7.37-6.89 (m, 7H, Ar), 6.62 (s, 1H, CH of thiazole), 3.22-3.20 (m, 6H, 2×OCH_3), 3.97 (s, 2H, CH_2); ^{13}C NMR (101 MHz, $CDCl_3$) δ ppm: 167.0, 164.7, 163.6, 151.7, 149.4, 143.7, 128.5, 120.8, 119.7, 109.7, 106.7, 100.6, 54.4, 37.6; HRMS (ESI) *m/z* for $C_{20}H_{17}N_5O_4S_2$ calculated: 455.0982, found: 455.0988.

***N*-(4-(3-Methoxyphenyl)thiazol-2-yl)-2-((5-(pyridine-4-yl)-1,3,4-oxadiazol-2-yl)thio)acetamide (3g):** Yield: 76%; off white solid; m.p.: 192-193 ºC; ^{1}H NMR (400 MHz, $CDCl_3$) δ ppm: 13.20 (s, 1H, NH), 7.81-7.29 (m, 8H, Ar), 6.42 (s, 1H, CH of thiazole), 3.97 (s, 2H, CH_2), 3.20 (s, 3H, CH_3); ^{13}C NMR (101 MHz, $CDCl_3$) δ ppm: 165.8, 164.7, 164.1, 160.8, 150.6, 149.8, 142.9, 137.6, 127.6, 121.5, 119.7, 111.7, 109.1, 101.7, 54.4, 39.1; HRMS (ESI) $C_{19}H_{15}N_5O_3S_2$ calculated: 425.4036, found: 425.4042.

2-(2-(2-((5-(Pyridine-4-yl)-1,3,4-oxadiazol-2-yl)thio)-acetamido)thiazol-4-yl)phenylacetate (3h): Yield: 72%; light yellow solid; m.p.: 202-203 ºC; ^{1}H NMR (400 MHz, $CDCl_3$) δ ppm: 12.52 (s, 1H, Ar), 7.94-7.35 (m, 8H, Ar), 6.74 (s, 1H, CH of thiazole), 3.97 (s, 2H, CH_2), 2.62 (s, 3H, CH_3); ^{13}C NMR (101 MHz, $CDCl_3$) δ ppm: 167.9, 165.4, 164.7, 164.6, 153.2, 150.3, 148.6, 143.7, 132.6, 129.2, 126.5, 123.5, 120.7, 105.1, 34.6, 26.1; HRMS (ESI) *m/z* for $C_{20}H_{15}N_5O_4S_2$ calculated: 453.3411, found: 453.3415.

2-((5-(Pyridine-4-yl)-1,3,4-oxadiazol-2-yl)thio)-*N*-(4-(*p*-tolyl)thiazol-2-yl)acetamide (3i): Yield: 78%; off white solid; m.p.: 196-197 ºC; ^{1}H NMR (400 MHz, $CDCl_3$) δ ppm: 12.69 (s, 1H, Ar), 7.94-7.35 (m, 8H, Ar), 6.74 (s, 1H, CH of thiazole), 3.97 (s, 2H, CH_2), 2.62 (s, 3H, CH_3); ^{13}C NMR (101 MHz, $CDCl_3$) δ ppm: 167.8, 164.7, 164.3, 151.4, 150.6, 145.6, 131.5, 129.2, 127.6, 122.7, 104.8, 36.5, 20.8; HRMS (ESI) *m/z* for $C_{19}H_{15}N_5O_2S_2$ calculated: 409.0007, found: 409.0008.

AChE inhibition: The AChE inhibitory activity of the synthesized derivatives **3a-i** was assessed against AChE enzyme from *Electrophorus electricus* by Ellman's method using done-

pezil as a reference compound [44]. A range of working solutions (µg/mL) were prepared using serial dilutions from stock solution (1 mg/mL) in DMSO. Acetylthiocholine iodide and 5,5′-dithiobis-2-nitrobenzoic acid (DTNB) were used as substrate and chromogenic reagent, respectively. A mixture of 5 mL phosphate buffer (0.05 M) with drug dilution, enzyme dilution (0.05 unit per tube), DTNB (0.01 M) each 1 mL followed by the addition of 2 mL of substrate (0.075 M) and incubated for 15 min at 37 ºC. Finally, the absorbance values of samples and control were recorded at 412 nm. The percentage of inhibition was calculated as: $A_{control} - A_{sample}/A_{control} \times 100$. Subsequently, IC_{50} values of final compounds were calculated.

DPPH assay: Radical scavenging capacity of compounds (**3a-i**) was evaluated by DPPH method [45,46]. In this assay, the decreased absorbance was monitored owing to the formation of DPPH-H (non-radical form). The 0.1 mM solution of DPPH was prepared in ethanol and then, 2 mL of DPPH solution was added to an aliquot (1 mL) of different diution of samples and reference (ascorbic acid) dilutions. The mixtures were mixed thoroughly and incubated in dark for 30-35 min. Finally, using a spectrophotometer, the absorbance value of samples and control were recorded at 517 nm. DPPH exhibits maximum absorbance at 517 nm. The decreased absorption after accepting radicals from antioxidant compounds was observed. Percentage radical scavenging was calculated by $A_{control} - A_{sample}/A_{control} \times 100$.

Docking study: The binding affinity and protein-ligand interactions of analogues were determined by conducting molecular docking with the target PDB 4EY7. Schrödinger suite 2022-1 version 13.1 using the Glide module in extra-precision (XP) mode was used to carry out molecular docking [47,48]. The structures (3D) of compounds were prepared using Marvin sketch software. The crystal structure of enzyme AChE (PDB 4EY7, resolution 2.35Å with no mutation) was retrieved from RCSB protein data bank (https://www.rcsb.org/Pdb/). The reference drug used for docking study is Donepezil. The LigPrep module was used to prepare ligands using force field OPLS_2005 (optimized potentials for liquid simulations) to retain chirality, ionization and generating low energy enantiomers. Protein preparation wizard was used to prepare protein by selecting assign bond order, adding hydrogen, filling in missing side chain/loops using prime, delete water from hetatoms to minimize protein using OPLS_2005 force field. The rationale behind selecting the glide module lies in the fact that it searches for the poses and ligand flexibility using systematic and simulation methods for accurate results. The acceptable superposition of co-crystallized ligand donepezil for PDB ID: 4EY7 with the docking pose (RMSD-0.8540) validate the study.

Molecular dynamic simulation: The GROMACS 2022.2 was used to carry out molecular dynamics (MD) simulation. The following steps were utilized.

Enzyme preparation: Pymol was used to export the three-dimensional (3D) models of ligand-protein complexes to the.pdb format. Through the use of molecular dynamic (MD) simulation within the GROMACS package program (version 2022.2) [49,50], the dynamic behaviour of the complexes was determined. While the Swiss Param server was used to produce ligand topologies, pdb2gmx was used to construct protein topologies using the CHARMM27 force field [51].

System setting for simulation: After the force field was applied, the complexes were introduced into the system. The solvation of the protein was performed using the TIP3P water model [52]. The protein was placed in a cubic box with dimensions greater than 1 nm from its edges and periodic boundary conditions were applied. The system was rendered inert by the process of energy minimization, utilizing the steepest descent technique and the introduction of Na^+ ions. Subsequently, a 100 ps NVT simulation was conducted at 300 K, followed by an NPT simulation to achieve equilibrium for the entire system. The Leapfrog algorithm was utilized in the constant-temperature, constant-pressure (NPT) ensemble to independently couple each constituent, such as the protein, ligand, water molecules, and ions [53]. The Berendsen temperature was adjusted to 1 and 2 for the pressure coupling constant in order to maintain the system in a stable environment with a temperature of 300 K and a pressure of 1 bar [54]. Ultimately, molecular dynamics simulation was conducted under conditions of constant temperature and pressure, specifically at 300 K for a duration of 100 ns. The time constant for pressure coupling was adjusted to 1 picosecond in order to maintain a constant pressure of 1 bar. The bond lengths were constrained using the LINCS algorithm [55]. The van der Waals and Coulomb interactions were limited to a distance of 1.2 nm. To reduce the inaccuracy caused by this limitation, the PME method [56] integrated into GROMACS was employed.

Simulation visualization and analysis: VMD (Visual Molecular Dynamics) 1.9.2. [57] was used to visualized the trajectory files and analyzed by indigenously developed tool HeroMDAnalysis [58] and Xmgrace 5.1.25 [59].

RESULTS AND DISCUSSION

Initially, aminothiazoles (**1a-i**) were synthesized by refluxing different substituted acetophenones (**a-i**) along with thiourea in the presence of iodine and triethylamine. The treatment of aminothiazoles (**1a-i**) with choloroacetylchloride in the presence of K_2CO_3 afforded intermediates (**2a-i**), which were further refluxed with compound **3** in the presence of K_2CO_3 in acetone to provide target compounds (**3a-i**) (**Scheme-I**).

The structures of all compounds were elucidated by ^{1}H NMR, ^{13}C NMR and mass spectrometric analysis. The stretching frequency due to NH and carbonyl of amide bond was obtained at 3439 and 1634 cm^{-1}, respectively. The band at 3058 cm^{-1} was assigned to aromatic =C-H stretching of aromatic ring. Further, IR spectrum of compound **3a** exhibits a band around 1535-1477 cm^{-1} to 1339-1271 cm^{-1} assignable to asymmetric and symmetric stretching of NO_2. In ^{1}H NMR of all the synthesized compounds, the presence of NH proton of amide group was confirmed by the appearance of singlet peak around δ 13.20-12.34 ppm and singlet peak around region δ 6.75-6.43 ppm confirmed the presence of CH of thiazole ring. The singlet peak around δ 4.13-3.85 ppm confirmed the formation of CH_2 linkage between thio and amide group. In ^{13}C NMR spectra of all compounds, signals for various carbons appeared in region

of δ 169.9-22.7 ppm. The *m/z* values in mass spectra of all compounds also confirmed the structure of desired compounds.

AChE inhibition: The AChE inhibitory activity of all synthesized derivatives (**3a-i**) was assessed against the AChE enzyme from *Electrophorus electricus* using Ellman's method, with donepezil serving as the standard reference [44]. Compounds **3a-i** exhibited inhibitory activity with IC_{50} values ranging from 0.35 μM to 15.69 μM, as shown in Table-1. Compound **3d** exhibited a high level of inhibitory activity, as indicated by its IC_{50} value of 0.35 μM. Compounds **3c** and **3e** exhibited notable inhibitory activity against AChE, with IC_{50} values of 1.85 μM and 2.98 μM, respectively. These values were compared to the reference compound donepezil, which had an IC_{50} value of 0.075 μM.

TABLE-1
AChE INHIBITORY AND ANTIOXIDANT ACTIVITY OF AMINOTHIAZOLE DERIVATIVES

Compound	(R)	IC_{50} (μM)	
		AChE	DPPH
3a	3-NO_2	8.33	3.03
3b	2,5-di-OCH_3	9.35	9.01
3c	4-Br	1.85	1.97
3d	2,4-di-Cl	0.35	1.93
3e	2-Cl	2.98	2.24
3f	3,4-di-OCH_3	6.52	1.12
3g	2-OCH_3	15.69	1.24
3h	2-$OCOCH_3$	56.50	22.18
3i	4-CH_3	9.09	0.89
Donepezil		0.075	–
Ascorbic acid		–	0.178

Compound **3d** (R = 2,4-dichloro) exhibited the highest level of activity, possibly attributed to the presence of electron withdrawing groups at the *ortho* and *para*-positions. The difference in inhibitory potential between compounds **3c** (R = 4-Br) and **3e** (R = 2-Cl) was primarily influenced by the substituent with lower electron withdrawing capability and the absence of chloro group at the *ortho*-position. Additionally, a reduction in inhibitory capacity was observed for compounds **3f** (IC_{50} = 6.52 μM), **3b** (IC_{50} = 9.35 μM) and **3g** (IC_{50} = 15.69 μM) that contained electron donating groups instead of electron withdrawing groups. The results showed that the most favourable substitution for AChE activity was the replacement of an electron withdrawing group at the *ortho*- and *para*-positions of the phenyl ring, which is substituted at the 4th position of the thiazole ring.

DPPH assay: Compounds **3a-i** exhibited radical scavenging capacity, as indicated by their IC_{50} values ranging from 0.89 μM to 22.18 μM (Table-1). The reference molecule, ascorbic acid, demonstrated its antioxidant activity with an IC_{50} value of 0.178 μM. Compound **3i** (R = 4-CH_3) had the highest antioxidant activity compared to other derivatives, with an IC_{50} value of 0.89 μM. The results indicated that the replacement of electron donating groups at the 2nd and 4th positions enhanced the antioxidant activity.

Docking study: The binding affinity and protein-ligand interactions of analogs were investigated by conducting molecular docking with the target PDB ID: 4EY7 [47,48]. Table-2 contains the binding affinity values for all the compounds that have been produced. The synthesized compounds exhibited binding affinities ranging from -7.739 to -10.787 kcal mol^{-1}. They had substantial binding interactions, such as hydrogen bonding, pi-pi stacking and halogen bonding, with the amino acid residues of the active region of the target enzyme (PDB 4EY7). Out of all the artificially created analogs, the analog **3d** had the highest binding score of -10.787 kcal mol^{-1}. Fig. 2 illustrates the probable binding mode and 2D interaction between the enzyme and the most potent compound **3d**. The carbonyl oxygen of compound **3d** formed a hydrogen bond with Tyr124, located at a distance of 2.41 Å. Additionally, the phenyl ring of the molecule exhibited pi-pi stacking with Trp286 residues, positioned at a distance of 4.11 Å.

TABLE-2
DOCKING ANALYSIS OF AMINOTHIAZOLE DERIVATIVES WITH AChE

Compd.	Docking score	Type of Interactions	Interaction with residues
3a	-8.371	H-bond	Tyr124
3b	-7.459	2 H-bond	Tyr124 & Phe295
3c	-9.332	3 H-bond	Tyr124 (2) & Tyr133
3d	-10.787	H-bond	Tyr124
		2 π-π stacking	Trp286 (2)
3e	-8.737	H-bond	Tyr124
3f	-8.844	3 π-π stacking	Trp286 (3)
3g	-8.743	H-bond	Tyr124
		5 π-π stacking	Trp86 (2), Trp286 (3)
3h	-7.739	2 H-bond	Tyr124
		6 π-π stacking	Trp86 (3), Trp286 (3)
3i	-8.979	H-bond	Tyr 124
		3 π-π stacking	Tyr337, Tyr341, Tyr124
Donepezil	-11.855	H-bond	Phe295
		π-π stacking	Trp86

The involvement of 2,4-dichloro substituted phenyl ring in establishing hydrophobic interaction may be contributing for better activity of compound **3d** as compare to compound **3e** (R = 2-Cl). The binding interactions of compounds **3h** (R = 2-$OCOCH_3$) and **3g** (R = 2-OCH_3) with residues of enzyme were nearly same. All the compounds may have exhibited higher inhibitory potential due to electrostatic contact with Tyr124 and hydrophobic interaction with Trp286 and Phe338 residues of the enzyme.

Molecular dynamic simulations of AChE in complex with donepezil and compound 3d: In order to understand the conformational changes and evaluatethe binding of donepezil (standard), Compound **3d** against AChE (PDB 4EY7), we have carried out molecular dynamic (MD) simulations for a period of 100 ns for three models namely, donepezil-4EY7, compound **3d**-4EY7 (Fig. 3). Their simulations were evaluated using various statistical parameters including H-bond interactions and its percentage occupancies over time.

RMSD analysis: RMSD analysis gives insights about any structural conformation that protein and ligand undergo during the simulation. The plateau in RMSD values (around 0.18 nm), indicating that the newly identified compound **3d** has interacted similarly to AChE as standard donepezil. Donepezil and comp-

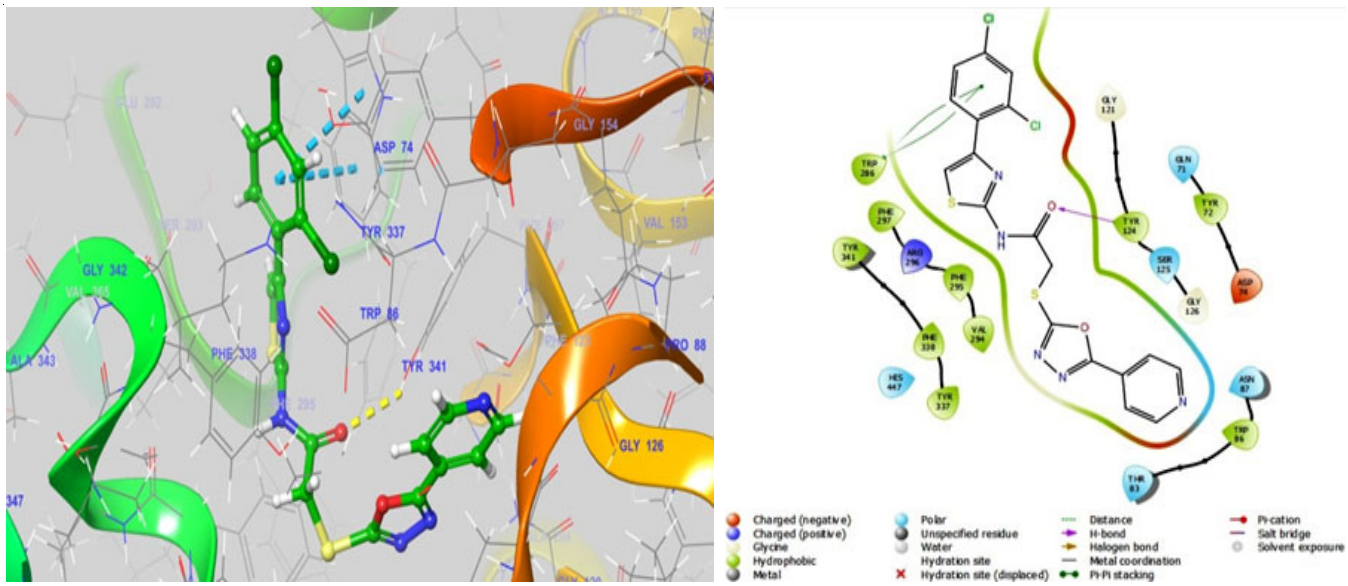

Fig. 2. Potential binding pose and 2D interaction diagram between AChE and most potent compound **3d** (H-bond-purple colour, π-π stacking-green colour)

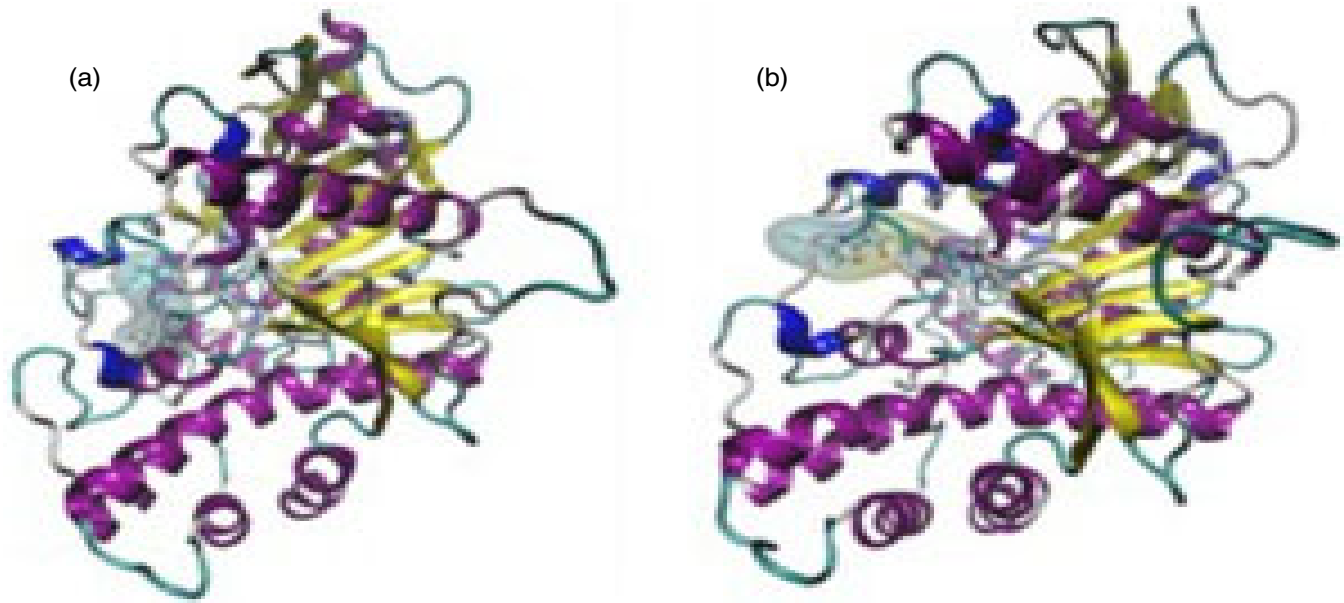

Fig. 3. Graphical representation of protein-ligand complexes: (a) donepezil-4EY7 and (b) compound **3d**-4EY7 where protein is shown in cartoon representation and the ligand is shown in CPK representation with transparent surface

ound **3d** have shown RMSD values of lower magnitude (less than 0.25 nm) which indicated their capability in binding AChE.

RMSF analysis: The multiplot for protein-RMSF (nm) *versus* residue number index describes fluctuation of less than 0.35 nm for most of the protein residues, which again indicated stability.

H-bond interaction: Herein, we have analyzed the H-bond interactions for the complexes of donepezil and compound **3d** with protein that are liable to disruption under dynamic conditions. The plot for the number of hydrogen bonds *vs.* time observed that compounds **3d** displayed comparatively good H-bond contacts during the simulation (Fig. 4). The percentage occupancies *vs.* the residues were calculated to access the residues involved in such interactions and their stabilities,

The histogram of percentage occupancies of the H-bond contacts formed by the two ligands (donepezil and compound **3d**). Fig. 5 has displayed the ability of donepezil to form a stable interaction with residue ASP74 of human AChE with occupancy of 14.17%. To our delight, compound **3d** has shown much stable H-bond interactions with the residues ASP74, TYR124 and TYR133, which were stable for 48.70, 19.57 and 13.21% duration of the simulation. The data predicted that compound **3d** can be more efficient in binding with target enzyme.

Conclusion

The thioacetamido-thiazole hybrid derivatives (**3a-i**) were sucessfully synthesized, characterized through IR, ^{1}H NMR, ^{13}C NMR and HRMS and evaluated for their AChE inhibitory

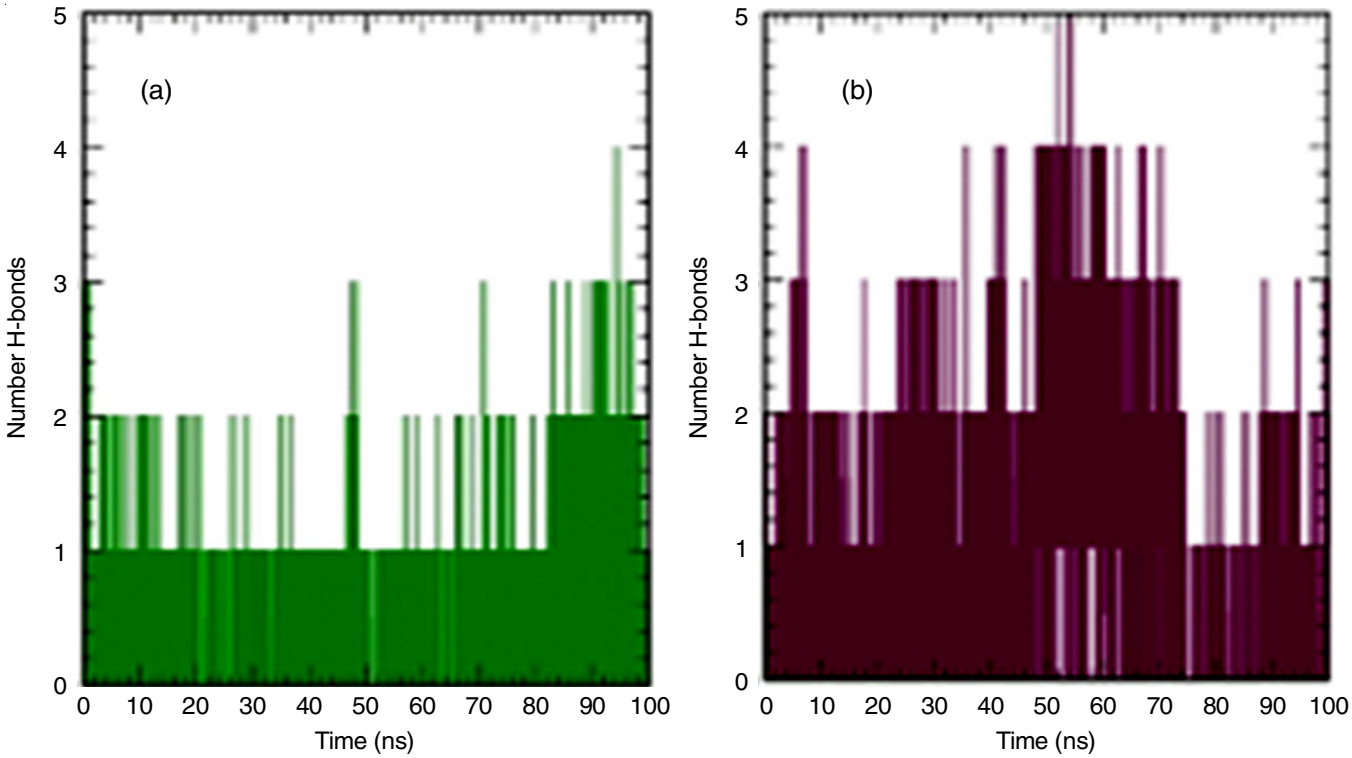

Fig. 4. Pictorial representation of the number of h-bond contacts formed by ligands (a) donepezil, (b) compound **3d** in complex with AChE (PDB ID: 4EY7)

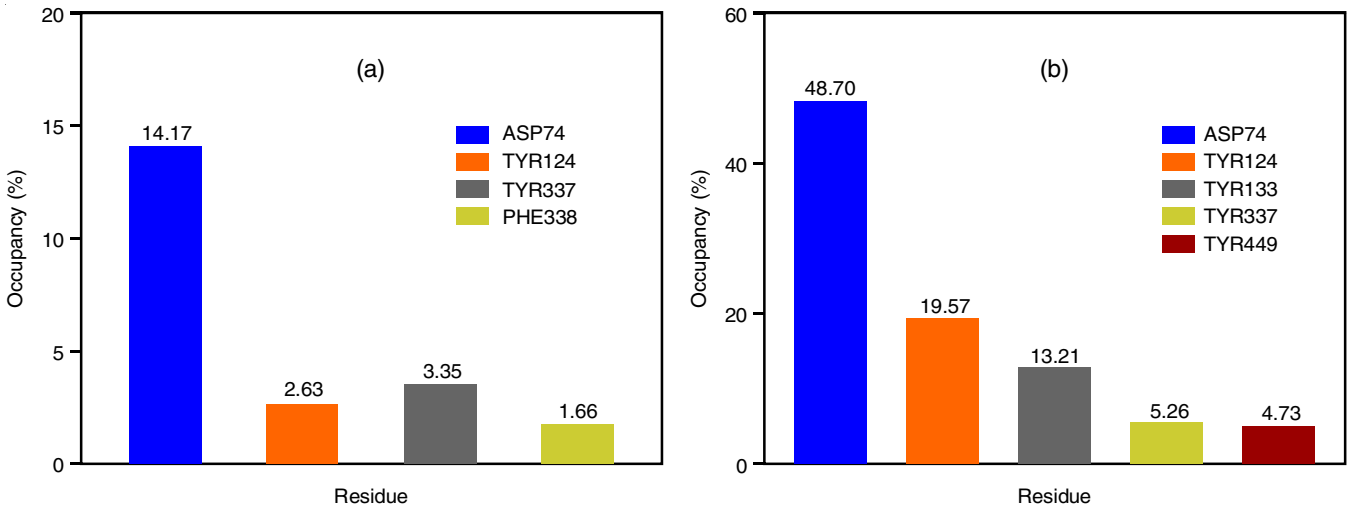

Fig. 5. Histogram representation of % occupancies of the h-bond protein-ligand contacts of (a) donepezil, (b) compound **3d** in complex with human acetylcholinesterase

and antioxidant activity. The results revealed that aminothiazole derivatives bearing oxadiazole moiety was synthesized in good yield. Compound **3d** exhibited the highest AChE inhibitory potential with IC_{50} = 0.35 µM. The best antioxidant potential was exhibited by compound **3i** with IC_{50} = 0.89 µM. Molecular docking observations revealed that the strong binding of these compounds with AChE is attributed to a high docking score and non-covalent (electrostatic and hydrophobic) interactions. Therefore, the novel synthesized compounds can be regarded as effective for the advancement of novel candidates against Alzheimer's disease.

ACKNOWLEDGEMENTS

One of authors (AS) is thankful to Panipat Institute of Engineering and Technology, Panipat, India for providing the infrastructure and other research facilities.

CONFLICT OF INTEREST

The authors declare that there is no conflict of interests regarding the publication of this article.

REFERENCES

1. R. Sengoku, *Neuropathology*, **40**, 22 (2020); https://doi.org/10.1111/neup.12626
2. P.S. Aisen and K.L. Davis, *Neurology*, **48(5suppl_6)**, 35S (1997); https://doi.org/10.1212/WNL.48.5_Suppl_6.35S
3. R. Hussain, H. Ullah, F. Rahim, M. Sarfraz, M. Taha, R. Iqbal, W. Rehman, S. Khan, S.A.A. Shah, S. Hyder, M. Alhomrani, A.S. Alamri, O. Abdulaziz and M.A. Abdelaziz, *Molecules*, **27**, 6087 (2022); https://doi.org/10.3390/molecules27186087
4. M.S. Uddin, A. Al Mamun, M.T. Kabir, M. Jakaria, B. Mathew, G.E. Barreto and G.M. Ashraf, *Mol. Neurobiol.*, **56**, 4925 (2019); https://doi.org/10.1007/s12035-018-1420-2
5. https://www.who.int/news-room/fact-sheets/detail/dementia
6. R.-M. Lu, Y.-C. Hwang, I.-J. Liu, C.-C. Lee, H.-Z. Tsai, H.-J. Li and H.-C. Wu, *J. Biomed. Sci.*, **27**, 1 (2020); https://doi.org/10.1186/s12929-019-0592-z
7. S.P. Yun, D. Kim, S. Kim, S.M. Kim, S.S. Karuppagounder, S.-H. Kwon, S. Lee, T.-I. Kam, S. Lee, S. Ham, J.H. Park, V.L. Dawson, T.M. Dawson, Y. Lee and H.S. Ko, *Mol. Neurodegener.*, **13**, 1 (2018); https://doi.org/10.1186/s13024-017-0233-5
8. B.L. Sun, W.W. Li, C. Zhu, W.-S. Jin, F. Zeng, Y.-H. Liu, X.-L. Bu, J. Zhu, X.-Q. Yao and Y.-J. Wang, *Neurosci. Bull.*, **34**, 1111 (2018); https://doi.org/10.1007/s12264-018-0249-z
9. S.E. Swalley, *Bioorg. Med. Chem.*, **28**, 115239 (2020); https://doi.org/10.1016/j.bmc.2019.115239
10. J. Fang, Y. Li, R. Liu, X. Pang, C. Li, R. Yang, Y. He, W. Lian, A.-L. Liu and G.-H. Du, *J. Chem. Inf. Model.*, **55**, 149 (2015); https://doi.org/10.1021/ci500574n
11. P. Zhang, S. Xu, Z. Zhu and Z. Xu, *Eur. J. Med. Chem.*, **176**, 228 (2019); https://doi.org/10.1016/j.ejmech.2019.05.020
12. S.-Y. Hung and W.-M. Fu, *J. Biomed. Sci.*, **24**, 47 (2017); https://doi.org/10.1186/s12929-017-0355-7
13. C. Ballard, S. Gauthier, A. Corbett, C. Brayne, D. Aarsland and E. Jones, *Lancet*, **377**, 1019 (2011); https://doi.org/10.1016/S0140-6736(10)61349-9
14. G. Marucci, M. Buccioni, D.D. Ben, C. Lambertucci, R. Volpini and F. Amenta, *Neuropharmacology*, **190**, 108352 (2021); https://doi.org/10.1016/j.neuropharm.2020.108352
15. Y. Zhao and B. Zhao, *Oxid. Med. Cell. Longev*., **2013**, 316523 (2013); https://doi.org/10.1155/2013/316523
16. M.T. Islam, *Neurol. Res.*, **39**, 73 (2017); https://doi.org/10.1080/01616412.2016.1251711
17. M. Gubandru, D. Margina, C. Tsitsimpikou, N. Goutzourelas, K. Tsarouhas, M. Ilie, A.M. Tsatsakis and D. Kouretas, *Food Chem. Toxicol.*, **61**, 209 (2013); https://doi.org/10.1016/j.fct.2013.07.013
18. D.J. Hardy and D.J. Selkoe, *Science*, **297**, 353 (2002); https://doi.org/10.1126/science.1072994
19. B.N. Saglik, D. Osmaniye, U.A. Çevik, S. Levent, B.K. Çavusoglu, Y. Özkay and Z.A. Kaplancikli, *Molecules*, **25**, 4312 (2020); https://doi.org/10.3390/molecules25184312
20. B. Kilic, M. Bardakkaya, R. Ilikci Sagkan, F. Aksakal, S. Shakila and D.S. Dogruer, *Bioorg. Chem.*, **131**, 106322 (2023); https://doi.org/10.1016/j.bioorg.2022.106322
21. H.A. Ghabbour, A.A. Kadi, K.E. ElTahir, R.F. Angawi and H.I. El-Subbagh, *Med. Chem. Res.*, **24**, 3194 (2015); https://doi.org/10.1007/s00044-015-1371-3
22. E.O. Al-Tamimi and H.F. Abdul Mahdi, *Int. J. Curr. Microbiol. Appl. Sci.*, **5**, 1 (2016); https://doi.org/10.20546/ijcmas.2016.508.001
23. K. Rehse and T. Baselt, *Arch. Pharm. (Weinheim)*, **341**, 645 (2008); https://doi.org/10.1002/ardp.200700046
24. A.M. Mohamed, N.A. Abdel-Hafez, A.F. Kassem, E.M.H. Abbas and M.M. Mounier, *Russ. J. Gen. Chem.*, **87**, 2391 (2017); https://doi.org/10.1134/S1070363217100218
25. C.I. Lino, I. Gonçalves de Souza, B.M. Borelli, T.T. Silvério-Matos, I.N. Santos Teixeira, J.P. Ramos, E. Maria de Souza Fagundes, P. de Oliveira Fernandes, V.G. Maltarollo, S. Johann and R.B. de Oliveira, *Eur. J. Med. Chem.*, **151**, 248 (2018); https://doi.org/10.1016/j.ejmech.2018.03.083
26. J.A. Kaplancikli, G. Turan-Zitouni, G. Revial and K. Guven, *Arch. Pharm. Res.*, **27**, 1081 (2004); https://doi.org/10.1007/BF02975108
27. M. Modriæ, M. Bozicevic, I. Faraho, M. Bosnar and I. Skoric, *J. Mol. Struct.*, **1239**, 130526 (2021); https://doi.org/10.1016/j.molstruc.2021.130526
28. I.N. Korkmaz, *Biotechnol. Appl. Biochem.*, **70**, 659 (2023); https://doi.org/10.1002/bab.2388
29. P. Arora, R. Narang, S.K. Nayak, S.K. Singh and V. Judge, *Med. Chem. Res.*, **25**, 1717 (2016); https://doi.org/10.1007/s00044-016-1610-2
30. C.B. Mishra, S. Kumari and M. Tiwari, *Eur. J. Med. Chem.*, **92**, 1 (2015); https://doi.org/10.1016/j.ejmech.2014.12.031
31. M.F. Arshad, A. Alam, A.A. Alshammari, M.B. Alhazza, I.M. Alzimam, M.A. Alam, G. Mustafa, M.S. Ansari, A.M. Alotaibi, A.A. Alotaibi, S. Kumar, S.M.B. Asdaq, M. Imran, P.K. Deb, K.N. Venugopala and S. Jomah, *Molecules*, **27**, 3994 (2022); https://doi.org/10.3390/molecules27133994
32. N.H. Elghazawy, D. Zaafar, R.R. Hassan, M.Y. Mahmoud, L. Bedda, A.F. Bakr and R.K. Arafa, *ACS Chem. Neurosci.*, **13**, 1187 (2022); https://doi.org/10.1021/acschemneuro.1c00766
33. B.F.D. Gatphoh, N.N. Aggarwal, H. Kumar and B.C. Revanasiddappa, *Thai J. Pharm. Sci.*, **45**, 492 (2021).
34. G. Sahin, E. Palaska, M. Ekizoglu and M. Özalp, *Il Farmaco*, **57**, 539 (2002); https://doi.org/10.1016/S0014-827X(02)01245-4
35. S.S. Thakkar, P. Thakor, H. Doshi and A. Ray, *Bioorg. Med. Chem.*, **25**, 4064 (2017); https://doi.org/10.1016/j.bmc.2017.05.054
36. M.A. Tantray, I. Khan, H. Hamid, M.S. Alam, A. Dhulap and A. Kalam, *Bioorg. Chem.*, **77**, 393 (2018); https://doi.org/10.1016/j.bioorg.2018.01.040
37. A.G. Banerjee, N. Das, S.A. Shengule, R.S. Srivastava and S.K. Shrivastava, *Eur. J. Med. Chem.*, **101**, 81 (2015); https://doi.org/10.1016/j.ejmech.2015.06.020
38. B. Yadagiri, S. Gurrala, R. Bantu, L. Nagarapu, S. Polepalli, G. Srujana and N. Jain, *Bioorg. Med. Chem. Lett.*, **25**, 2220 (2015); https://doi.org/10.1016/j.bmcl.2015.03.032
39. W. Wu, Q. Chen, A. Tai, G. Jiang and G. Ouyang, *Bioorg. Med. Chem. Lett.*, **25**, 2243 (2015); https://doi.org/10.1016/j.bmcl.2015.02.069
40. P. Mishra, P. Sharma, P.N. Tripathi, S.K. Gupta, P. Srivastava, A. Seth, A. Tripathi, S. Krishnamurthy and S.K. Shrivastava, *Bioorg. Chem.*, **89**, 103025 (2019); https://doi.org/10.1016/j.bioorg.2019.103025
41. A. Soni, A. Kumar, V. Kumar, R. Rawat and V. Eyupoglu, *Future Med. Chem.*, **16**, 513 (2024); https://doi.org/10.4155/fmc-2023-0290
42. N. Singh, U.S. Sharma, N. Sutar, S. Kumar and U.K. Sharma, *J. Chem. Pharm. Res.*, **2**, 691 (2010).
43. H. Bayrak, A. Demirbas, N. Demirbas and S.A. Karaoglu, *Eur. J. Med. Chem.*, **44**, 4362 (2009); https://doi.org/10.1016/j.ejmech.2009.05.022
44. E. Garibov, P. Taslimi, A. Sujayev, Z. Bingol, S. Çetinkaya, I. Gulçin, S. Beydemir, V. Farzaliyev, S.H. Alwasel and C.T. Supuran, *J. Enzyme Inhib. Med. Chem.*, **31(sup3)**, 1 (2016); https://doi.org/10.1080/14756366.2016.1198901
45. L.M. Magalhães, M.A. Segundo, S. Reis and J.L.F.C. Lima, *Anal. Chim. Acta*, **613**, 1 (2008); https://doi.org/10.1016/j.aca.2008.02.047
46. M. Elmastas, I. Gülcin, S. Beydemir, Ö. Irfan Küfrevioglu and H.Y. Aboul-Enein, *Anal. Lett.*, **39**, 47 (2006); https://doi.org/10.1080/00032710500423385
47. Schrödinger Suite Release, 2018-3: Glide. New York, NY, Schrödinger, LLC (2018).
48. R.A. Friesner, R.B. Murphy, M.P. Repasky, L.L. Frye, J.R. Greenwood, T.A. Halgren, P.C. Sanschagrin and D.T. Mainz, *J. Med. Chem.*, **49**, 6177 (2006); https://doi.org/10.1021/jm051256o

49. H. Bekker, H.J.C. Berendsen, E.J. Dijkstra, S. Achterop, R. Vondrumen, D. Vanderspoel, A. Sijbers, H. Keegstra and M.K.R. Renardus, GROMACS-A Parallel Computer for Molecular-Dynamics Simulations, In 4th International Conference on Computational Physics, World Scientific Publishing, Singapore, pp. 252-256 (1993).
50. A. Ganesan, M.L. Coote and K. Barakat, *Drug Discov. Today*, **22**, 249 (2017); https://doi.org/10.1016/j.drudis.2016.11.001
51. N. Schmid, A.P. Eichenberger, A. Choutko, S. Riniker, M. Winger, A.E. Mark and W.F. van Gunsteren, *Eur. Biophys. J.*, **40**, 843 (2011); https://doi.org/10.1007/s00249-011-0700-9
52. P. Mark and L. Nilsson, *J. Phys. Chem. A*, **105**, 9954 (2001); https://doi.org/10.1021/jp003020w
53. W.F. Van Gunsteren and H.J.C. Berendsen, *Mol. Simul.*, **1**, 173 (1988); https://doi.org/10.1080/08927028808080941
54. H.J.C. Berendsen, D. van der Spoel and R. van Drunen, *Comput. Phys. Commun.*, **91**, 43 (1995); https://doi.org/10.1016/0010-4655(95)00042-E
55. B. Hess, H. Bekker, H.J.C. Berendsen and J.G.E.M. Fraaije, *J. Comput. Chem.*, **18**, 1463 (1997); https://doi.org/10.1002/(SICI)1096-987X(199709)18:12<1463::AID-JCC4>3.0.CO;2-H
56. M. Di Pierro, R. Elber and B. Leimkuhler, *J. Chem. Theory Comput.*, **11**, 5624 (2015); https://doi.org/10.1021/acs.jctc.5b00648
57. W. Humphrey, A. Dalke and K. Schulten, *J. Mol. Graph.*, **14**, 33 (1996); https://doi.org/10.1016/0263-7855(96)00018-5
58. R. Rawat, K. Kant, A. Kumar, K. Bhati and S.M. Verma, *Future Med. Chem.*, **13**, 447 (2021); https://doi.org/10.4155/fmc-2020-0191
59. A. Vaught and J. Linux (1996); www.linuxjournal.com/article/1218